Case Studies in Thermal Engineering 49 (2023) 103310

Contents lists available at ScienceDirect

Case Studies in Thermal Engineering

journal homepage: www.elsevier.com/locate/csite

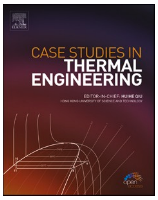

Experimental study with thermal and economical analysis for some modifications on cylindrical sector and double slope, single basin solar still

Mahmoud S. El-Sebaey [a,*], Asko Ellman [b], Ahmed Hegazy [a], Fadl A. Essa [c]

[a] *Mechanical Power Engineering Department, Faculty of Engineering, Menoufia University, Shebin El-Kom, 32511, Egypt*
[b] *Faculty of Engineering and Natural Sciences, Tampere University, Finland*
[c] *Mechanical Engineering Department, Faculty of Engineering, Kafrelsheikh University, Kafrelsheikh, 33516, Egypt*

ARTICLE INFO

Handling Editor: Huihe Qiu

Keywords:
Double slope solar still
Semi-cylinderical solar still
Production rate
Solar still modifications and efficiency

ABSTRACT

Solar stills are considered one of the most thermally eco-friendly and promising solutions for producing potable water in sunny and arid regions. However, they suffer from a disadvantage in terms of their low productivity. Therefore, this study aims to investigate the performance of cylindrical sector solar stills and compare them with double-slope solar stills. The study also presents the enhanced performance of a thermo-economic system by integrating cost-effective and readily available materials. The experiments were conducted in Egyptian climate conditions, with a water depth of 2 cm in the stills basin, using different materials. Under the same operating conditions, the results showed that the accumulated productivities of the cylindrical sector solar stills (CSSS) and double slope solar stills (DSSS), using black fiber and black dye, were 3514 ml/m^2 and 3029 ml/m^2, respectively, representing an increase of 16.01%. Furthermore, the daily thermal efficiency of the CSSS and DSSS, using black fiber and black dye, were 30.42% and 26.32%, respectively, showing an increase of 15.58%. The cost per liter (CPL) of potable water produced by CSSS, using black dye with black natural-fiber, was approximately 0.0119 US$/L, while it was 0.0137 US$/L for DSSS. Additionally, the payback periods for CSSS and DSSS were 92 days and 106 days, respectively. In all scenarios studied, the daily accumulated productivities and thermal efficiency of CSSS were greater than those of DSSS.

1. Introduction

According to UNICEF reports about water 2021, the water consumption was steadily raising with 1% all over the world from 1980 because of the rapid population growth, change in water consumption patterns and socio economic development by the people [1]. Over half of the world's population is predicted to be suffering from freshwater shortage by 2025. Potable water withdrawals for home, agricultural and industrial purposes surpass 4.6 trillion cubic meter yearly, and this consumption is expected to rise by roughly 25% by 2050 [2]. Thus, meeting this growing demand will be a critical problem in the twenty-first century. Energy, water and climate challenges are intertwined variables which affect all of human activities on the planet, and they are quickly attractive the most collective topics in energy study [3].

Due to the scarcity of freshwater, sea water could play an important role in drinking and other applications. In the form of total

---

[*] Corresponding author.

E-mail address: eng_mahmoudelsebaey@yahoo.com (M.S. El-Sebaey).

https://doi.org/10.1016/j.csite.2023.103310
Received 17 October 2022; Received in revised form 10 July 2023; Accepted 15 July 2023

dissolved solids (TDS), sea water has a high salinity (35,000-45,000 ppm) [4]. So, for using this seawater, it must be desalinated. Every day, more than 15,000 desalination plants throughout the world output about 37 million cubic meter of fresh water. More than 52% of this capacity is in the Middle East. Some efforts were recently made to yield fresh water from contaminated and saltwater by means of solar distillation [5], membrane technology [6] and other technologies [7].

Solar stills are a basic structure to fabricate; eco-friendly; simple to work; and it may be swiftly used by anyone when potable water is limited. But, the distillate output and efficiency are insufficient. This provided scientists with a compelling reason to investigate the aspects that influence its performance, such as climatic, design, and operational circumstances [8,9and10]. So, there are a lot of studies over the world to improve the efficiency and freshwater yield of the solar stills by modifying their design, such as single slope [11], double slope [12], single-basin, double-basin [13], triple-basin [14], hemispherical [15] spherical stills [16], pyramid stills [17and18], tubular stills [19], single effect, multi-effect [20] and stepped stills [21and22]. In addition, the still's absorber basin is constantly updated to improve evaporation rate, such as trays [23], absorber coatings [24], inclined [25], corrugated [26] and wick [27]. Also, energy-storage materials such as nanoparticles [28and29], floating aluminum sheet [30], solar ponds [31], desiccant [32], phase change materials [33], glass cooling [34], volcanic rocks [35], rotating belts [36], fins [37], dyes [38], reflectors [39], parabolic trough collector [40] sun-tracking systems [41] and others frequently involve more space which are more complicated and consequently the increment on thermal performance may well not offset due to extra required costs. The primary goal of all of these varied designs and adjustments was to increase the solar still's output yield.

Several operating and geometrical parameters like; solar irradiation intensity, ambient temperature, surrounding wind velocity, exposed area, and depth of water have an important influence on the daily output of the solar still [42]. The amount of solar intensity irradiated to solar still can be raised with increasing of the surface cover area. The configuration of the condensing cover has an important influence on the thermal performance; i.e. raising the quantity of solar energy captured by solar still. Various geometry of the cover plate as double, single, and curve of the solar still were investigated. The results of the experimental works show that the maximum daily output was achieved at the curved cover of the solar still compared to others [43].

Potable water is produced from industrial effluents by utilizing a fined solar still integrated by sand and sponge. Utilizing fins in the basin raise the evaporating rate because of raising the exposed heat transfer area which consequently improves the basin-type solar still thermal performance. The fin material effect; (glass; aluminum; copper; iron; and stainless steel) on the solar still thermal performance was experimentally conducted [44]. The results illustrated that the material of the fin does not significantly affect on the thermal performance. The daily yield for the finned basin-type of solar still made of glass was achieved 5.1 kg/m^2.day which show 16.3% increment in comparison to un-finned solar still. An experimental and numerical study shows that the daily yield is raised by rising the number of fins on fined double solar still. In addition, results show that the distance among the fins has not sufficient important on the daily yield [45]. The numerical study on finned solar still indicated that the heat transfer coefficient from the basin was raised by 3.6% over the conventional one. Also, the results of the integrated fins at the basin improved the thermal efficiency and daily productivity experimentally by 23.5% and 11.8%, respectively [46]. A pin fin absorber in solar still improved its yield by 14.3% compared with the conventional type [47]. The average output of the solar still by using fins made from graphite plate and magnet in the still basin was raised by 23.8% in comparison with the conventional one [48].

Solar still with a basin coated with black dye to enable absorbing the sun rays [49]. Black dye was found having a memorable influence on rising the solar stills productivity [50] while, the influence of different pigments changes in proportion with colours intensity [51].

It has been recognized that there is a trade-off between the thermal efficiency and exergetic efficiency of passive and active; DSSS [52]. Experimental results illustrated that the passive type still thermal efficiency is greater than of the active double slope; solar still while the inverse is achieved at the concept of the exergetic efficiency. On a seasonal base, the mass productivity of DSSS was higher than the pyramidal-shaped as well as single slope; solar stills [53]. The daily yield of double basin of DSSS was increased by 17.38% over the conventional still at lowest water depth of 1 cm [54].

Based on the literature study, the limitations of the double slope solar still, such as lower productivity, thermal and exergy efficiencies, and higher production costs due to shadow effects, have prompted to consider a new design of a cylindrical sector solar still incorporating black Lupha to enhance evaporation. The main objective of this study is to increase the daily productivity of the modified cylindrical sector solar still while simultaneously reducing the CPL for producing potable water.

The present paper presents an experimental study with thermal and economical analysis, focusing on modifications made to a cylindrical sector single-basin solar still. The study aims to demonstrate the operational characteristics of the proposed configurations under various operating conditions. Additionally, a comparison is made between the performance of the proposed configuration and that of the conventional double slope solar still to evaluate its practical feasibility. In summary, the objectives of this research can be summarized as follows:

1. The primary objective of this study is to develop and construct a Cylindrical Sector Solar Still (CSSS) along with a comparable Double Slope Solar Still (DSSS). The cylindrical shape is utilized as a condensing cover in the CSSS to maximize solar energy absorption and minimize shadowing effects caused by the cover of the solar still.
2. To examine the effects of incorporating fins and black dye on the thermal performance of the solar stills.
3. To examine the effect of incorporating dried black Luffa acutangula fibers into the basins of the solar stills, the wet surface area across their porous structure was increased. This enhancement is anticipated to lead to an accelerated evaporation rate of water from the basin.

2. Methodology

2.1. Test-rig description

A schematic view of cylindrical sector solar still [CSSS] is indicated in Fig. 1. The basin of the still's was made from 1.5 mm thickness of galvanized steel and the base was coated in black to raise the absorptivity and reduce the emissivity of the incident radiation, its inner dimension was taken as 1000 mm in width and 1000 mm in length as well as 100 mm high, with 1 m^2 total basin base area. To limit the heat loss to the atmosphere, the basin was insulated with a 50 mm thickness of sawdust. The inner side walls with a height of 40 mm was painted in black to act as an absorbent material to able absorb the largest possible quantity of global solar radiation while the other 60 mm was painted by white in order to reflect the global irradiation falling on it to the basin base. A cylindrical sector cover lying on the top of the solar still was constructed and shaped from a 1.5 mm polycarbonate sheet, the cylindrical chord was taken as 1000 mm and segment height of 289 mm, the segment height represents the height of the corresponding DSSS that its cover has a tilt angle of 30 degrees. A schematic view of the DSSS with the same basin dimensions and characteristics of CSSS is presented in Fig. 2.

For the two tested stills, the condensate water was collected into two measuring cylinders of 1000 ml capacity to measure freshwater productivity, by two semi-cylindrical 1-inch tubes which have a 1000 mm length, and to keep the water level at 20 mm and 40 mm inside the basins, the evaporative water was constantly compensated by a tank filled with saline water (35000 ppm). The tank was placed at a higher level than the basins. To assure the stability of the water level inside the basins a water weighing scale was used.

Fig. 3 exhibits the test-rig photograph. The two tested stills models were carried on a metal chassis made of 4 mm thick, 30 mm height and its outer dimensions are 1100 mm in length and 1100 mm in width, and 4 metal legs with a height of 600 mm. The metal chassis was also coated with an anti-corrosion paint.

Fig. 4-A shows a photographic view of the various materials that were used in this research, such as fins, black dye and dried black Luffa acutangula fibres. To enhance the thermal conductivity, potable water yield, and increase the absorbing surface area of the basin, 9 longitude fins of 1000 mm in length and 20 mm in height were welded to the basin at equal distances (The space between fins centers is 100 mm), the fins are made from galvanized steel with of 1 mm thickness for the two tested stills as shown in the schematic view of Fig. 4-B.

Fig. 4-C shows the number of natural Luffa acutangula fiber inside the basins of the CSSS and DSSS to increase the solar still yield, the absorption of water, porosity and retention of natural fiber led to increase the absorption surface area. The natural fiber was coated in black for increasing the absorptivity and reducing the emissivity. The availability, environmental aspects and minimum price were significant factors that driven to select the natural-fiber.

The black basin absorbs most of global solar irradiation incident, depending on the heat transfer efficacy among the galvanized steel base and the water, a part of heat is transferred through the convection to the water; and the exist part is lost through the insulation with conduction. So that with adding a black dye with the water, the water absorbs a huge value of the incident global solar irradiation and a little part was absorbed by the basin base. The water direct heating and the smaller basin losses led to reaching a higher temperature, and higher distillate fresh-water. The CSSS and DSSS were orintated to the direction of south to draw the

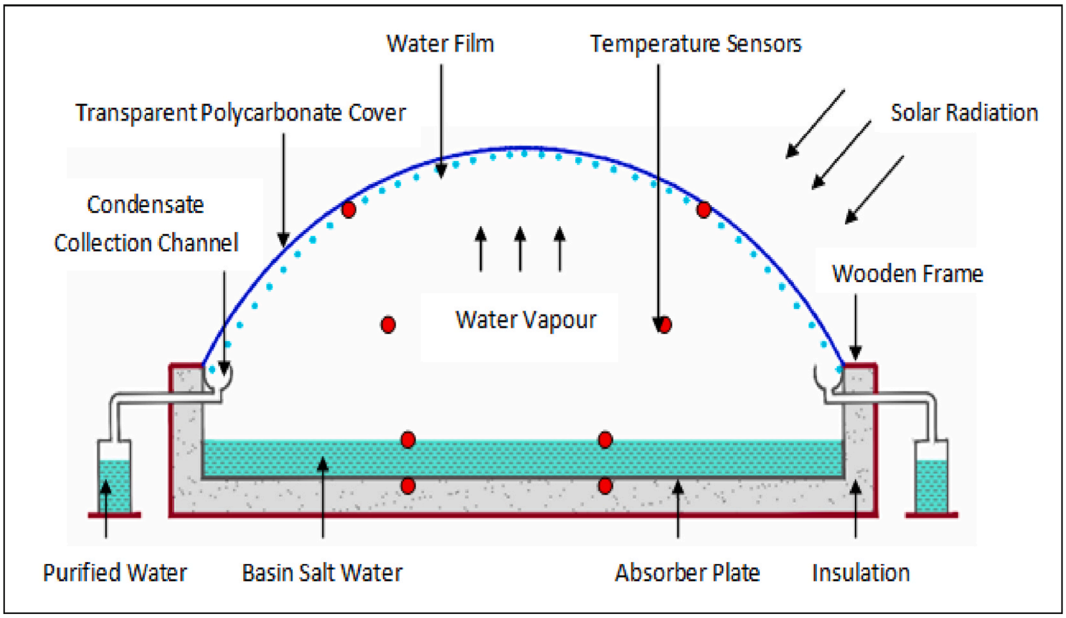

Fig. 1. A schematic view of the CSSS, Cylindrical Sector Solar Still.

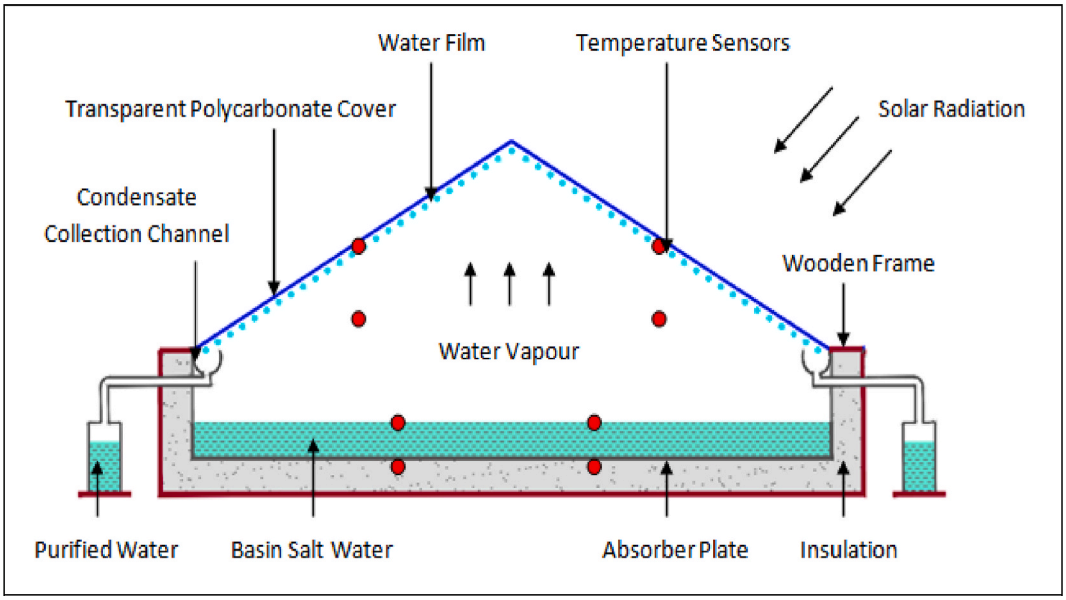

Fig. 2. A schematic view of the DSSS, Double Slope Solar Still.

Fig. 3. A photograph of the Test-rig.

maximum solar irradiation through the experiments.

2.2. Measuring instruments and uncertainty analysis

The experimental test-rig included appropriate measuring instruments for recording the changes in various parameters at hourly intervals. To record the variation of the temperature by time, calibrated thermocouples of K-type (Range of -210 to +750 °C; Accuracy ±0.05 °C; Uncertainty 1.3%) were distributed in many places inside the two tested stills to measure the water vapor temperature, the temperature around the polycarbonate cover surface, and measuring the temperature of the basin surface, fins, natural fiber, basin's slain water temperature with and without dye. And the ambient dry bulb temperature was recorded by calibrated mercury thermometer (Range of 0–100 °C; Accuracy ±0.5 °C; Uncertainty 1.5%). To take into account the effect of wind on the stills performance, an digital GM817 vane-type anemometer (Range of 0.1–25 m/s; Accuracy ± 0.1 m/s; Uncertainty 1.2%) was utilized. In addition, to measure the global solar irradiance falling on the CSSS and DSSS a calibrated digital Pyranometer (Range of 0–2000 W/m^2; Accuracy

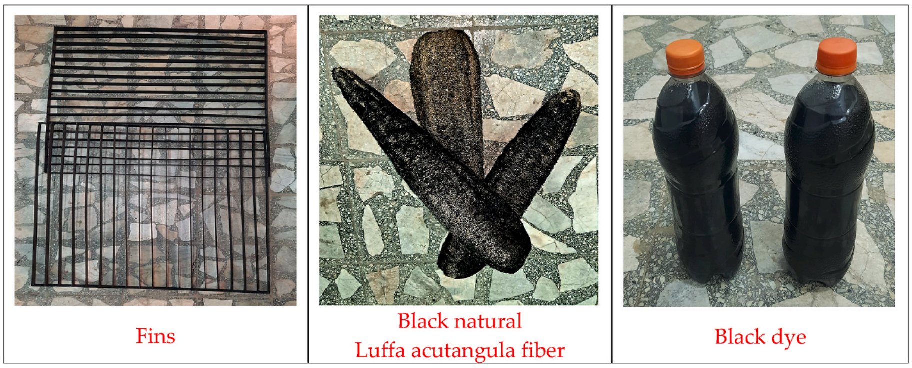

Fig. 4-A. A photograph of materials used.

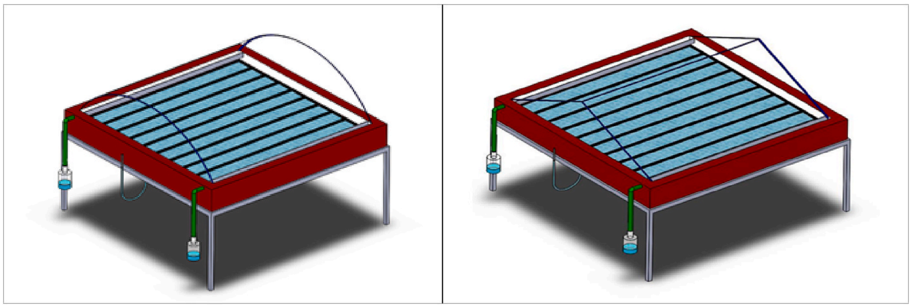

Fig. 4-B. Anthropomorphic view of the CSSS and DSSS with Fins.

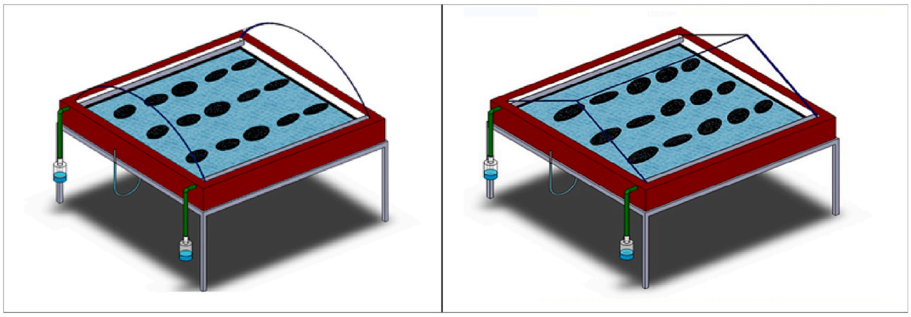

Fig. 4-C. Anthropomorphic view of the CSSS and DSSS with Luffa Fiber.

±10 W/m^2; Uncertainty 1.6%) was utilized and to measure the fresh water output, an graduated flash (Range of 0–500 ml; Accuracy ±1 ml; Uncertainty 0.5%) was used.

To determine the uncertainty of the X function; the coming equation was utilized:

$$w_x = \left[\left(\frac{\partial X}{\partial x_1}\right)^2 .{wx_1}^2 + \left(\frac{\partial X}{\partial x_2}\right)^2 .{wx_2}^2 + \ldots\ldots\ldots\ldots + \left(\frac{\partial X}{\partial x_n}\right)^2 .{wx_n}^2\right]^{\frac{1}{2}} \tag{1}$$

If w_x is the uncertainty diffusion for an x value, w represents the uncertainty of the measured parameter, and x_n represents the interest parameter. The hourly output with water depth function in the still basin can be written as $m = f(d)$. So, the output uncertainty is:

$$w_m = \left[\left(\frac{\partial m}{\partial d}\right)^2 .{w_d}^2\right]^{\frac{1}{2}} \tag{2}$$

Furthermore, the thermal efficiency uncertainty in (η_{th}) is:

$$w_{\eta_{th}} = \left[\left(\frac{\partial \eta_{th}}{\partial m} \right)^2 . {w_m}^2 + \left(\frac{\partial \eta_{th}}{\partial I(t)} \right)^2 . {w_{I(t)}}^2 \right]^{\frac{1}{2}} \tag{3}$$

Therefore, the Uncertainty of daily yield and the efficiency were about ±1.3% and ±2.4%, respectively.

2.3. Experimental procedure

The experimental used test-rig was assembled and installed at shebin-Elkom, (longitude 31.01° E and latitude of 30.5° N), Egypt. The experiments were performed during July and August 2021. The discussed instruments above with suitable uncertainties have been used for recording the affected parameters values on the stills performance each an hour. Five experimental tests were performed during July and August 2021 to achieve the best performance of the tested CSSS and DSSS. The tests were started at 7:00 to 20:00 over a period of three days for each test to ensure the repeatability and there was no great variation in the yield through the experiments repetition and then one day off for cleaning and maintenance the stills before the next test. The water depth was fixed at 2 cm inside the stills basins. The following will mention these tests:

1. Salt water with finned Cylindrical Sector Solar Still and Double Slope Solar Still.
2. Salt water with black natural-fiber in CSSS and DSSS.
3. Salt water with black dye in CSSS and DSSS.
4. Salt water with black dye in finned CSSS and DSSS.
5. Salt water with black dye and black natural-fiber in CSSS and DSSS.

3. Thermal and economical analysis

3.1. Energy balance equations

3.1.1. Polycarbonate condensing cover

The Polycarbonate condensing cover equation of the energy balance for a unit area that heat exchanges between water and the environment for the CSSS and DSSS can be formed as:

$$m_{pc}.C_{pc}.\frac{\partial T_{pc}}{\partial t} = H_{pc}(t) + q_{cw} + q_{ew} + q_{rw} - q_{r,pc-sky} - q_{c,pc-a} \tag{4}$$

3.1.2. Water

The energy balance of the water for a unit area that exchanges heat between the basin base, polycarbonate condensing cover and environment for the CSSS and DSSS can be written as:

$$m_w.C_w.\frac{\partial T_w}{\partial t} = H_w(t) + q_{c,b-w} - q_{cw} - q_{ew} - q_{rw} \tag{5}$$

Where, $q_{c,b-w}$ is the rate of heat transfer by convective from the basin base to water and may be determined with the aid of the coming equations [55]:

$$q_{c,b-w} = h_{c,b-w}.(T_b - T_w) \tag{6}$$

$$h_{c,b-w} = 0.54.\frac{k_w.Ra_w^{1/4}}{L_w} \text{ for Ra} = 10^4 \text{to } 10^7 \tag{7}$$

$$h_{c,b-w} = 0.15.\frac{k_w.Ra_w^{1/3}}{L_w} \text{ for Ra} = 10^7 \text{to } 10^{11} \tag{8}$$

3.1.3. Basin

The basin equation of the energy balance for a unit area of the two tested stills can be established as:

$$m_b.C_b.\frac{\partial T_b}{\partial t} = H_b(t) - q_{c,b-w} - q_{b-a} \tag{9}$$

3.2. Thermal efficiency

The daily thermal efficiency (η_d), for the CSSS and DSSS was calculated by summing; the hourly yield ($\dot{M}_w$), multiplied with the water latent heat (L), and then divided on the summing of average global solar irradiation through the day I(t), multiplied with the whole area of the basin base (A) of the tested still [56]:

$$\eta_d = \frac{\sum \dot{M}_w.L}{A_b.\sum I(t)}.100 \tag{10}$$

3.3. Economic analysis

The cost per liter of produced by each of the tested CSSS and DSSS potable water is calculated using economic analysis. According to the literature of [57and58], the economic analysis is described as the following:

The cost per liter (CPL) for produced potable water per meter square of the basin base is determined by:

$$CPL = \frac{TC}{AY} \tag{11}$$

Where the TC is the total annual cost and can be calculated as:

$$TC = FC + MC - SF \tag{12}$$

The first annual cost (FC) was determined by:

$$FC = CF.P \tag{13}$$

$$CF = \frac{i.(1+i)^{l_s}}{(1+i)^{l_s} - 1} \tag{14}$$

The annual maintenance cost (MC) per year is determined using:

$$MC = (0.15).FC \tag{15}$$

The annual savage factor (SF) is defined by:

$$SF = FF.S \tag{16}$$

$$FF = \frac{i}{(1+i)^{l_s} - 1} \tag{17}$$

$$S = (0.2).P \tag{18}$$

Where, the AY is the average annual potable water yield and is figured by multiplying the average productivity that gained through a day with the number of days that the still operating in a year.

The payback period (PP) for the solar still is expressed as:

$$PP = (TC / NF).SODY \tag{19}$$

Where, NF is the net profit of the still and it is determined as:

$$NF = (MPPW - CPL).AY \tag{20}$$

Where, MPPW is the market price of the potable water and it is considered as 0.25 \$/lit.

4. Results and discussion

The performance of any tested solar still is directly influenced by the weather conditions; especially global solar radiation intensity, ambient temperature and wind speed. So, the experiments were conducted through clear sunny days from July 15 to August 15, 2021.

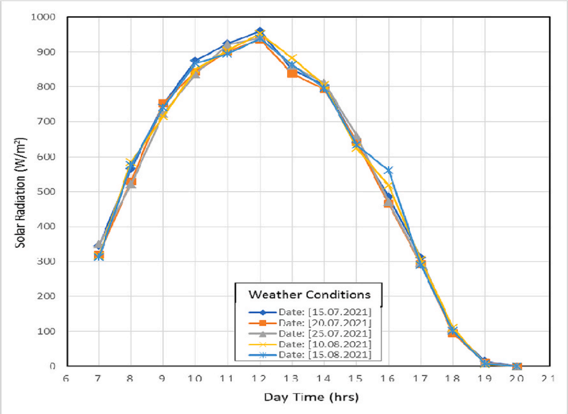

Fig. 5-A. Variations of total solar radiation intensity on horizontal surface through the experiments sunny days.

Fig. 5 presents the variation of total solar radiation, ambient temperature and wind speed through two different sunny tested days. It is noticed from Fig. 5-A that the solar intensities in the south-north orientations still had higher values and more stability and raised gradually with the daytime for all tested days from sunrise, reaching an maximum values of 960 W/m^2, 935 W/m^2, 940 W/m^2, 952 W/m^2 and 938 W/m^2 at 12:00, and then they decreased to the sunset. According to Fig. 5-B, throughout the daytime, the wind speed fluctuated among decrement and increment. At 7:00 and 20:00, the minimum and maximum wind speeds during the tested days were 0.2 and 2.8 m/s, respectively. Fig. 5-C shows the variation of the ambient temperatures during the experiments, and it was noticed that the highest temperature ranged from 24 °C at 7:00 a.m. to 40 °C at 14 p.m. which referred to thermal inertia of the mass for the ambient air. At 20:00, the lowest ambient temperature was dropped to 28.5 °C.

To be able to identify the performance of the tested SCSS and DSSS models, the variations of temperatures for the measured water and polycarbonate cover with the day time for 2 cm water depth are seen in Fig. 6-A and 6-B, respectively. From these Figs., it can be noticed that the water and polycarbonate temperatures of the cylindrical sector solar still [CSSS] are higher than DSSS at various tested modifications. The results indicate that the water temperatures gradually increased with the day time and get a peak value in afternoon time among 13:00 and 15:00. This is because of the increasing in the absorbed global solar intensity which surpasses the losses to the surrounding atmosphere. Furthermore, using the cylindrical sector cover for the modified solar still [CSS] prevent the shadow that caused in the case of Double Slope condensing cover. Also, it can be noticed that the maximum temperature for the water occurred at 14:00 for the both stills for the various modifications. This is because of the higher values of solar intensity received by the cylindrical sector cover than double slope cover and the facilitates of the cylindrical sector cover were admitting more quantities of solar intensity into the still. For the CSSS, the maximum recorded values of water temperatures were 67.5, 70.9, 73.2, 76.6 and 78.9 °C, while these values were 63.3, 65.4, 67.9, 71.6 and 74.7 °C for the DSSS, when using fins, black natural-fiber, black dye, black dye with fins and black dye with black natural-fiber, respectively.

Fig. 7-A and 7-B illustrate a comparison between the actual hourly and a cumulative rate of productivity for the various tested modifications of CSSS and DSSS with 2 cm water depth, respectively. At a higher temperature of the still water, extra evaporates of the water, and the water mass contained in the still air becomes greater. So, the maximum yield happens at the highest temperature of salt water in the still basin. From Fig. 7-A, the maximum actual values of the hourly productivity rate were recorded at 14:00 p.m. for all the considered modifications, which were 315, 330, 378, 399 and 413 ml/m^2.hr for the CSSS, while these values were 280, 295, 310, 338 and 348 ml/m^2.hr for the DSSS, when using fins, black natural-fiber, black dye, black dye with fins and black dye with black natural-fiber, respectively. After that, the production rate started to decrease till the sunset. Fig. 7-B shows the actual variation of the accumulated productivity of the CSSS and DSSS for the various materials used in the modifications of the basin of the tested stills. The accumulated productivity was higher for the two tested stills through the day time with using black dye and black fiber in the basin. The results suggests that the experimental accumulated productivities of the CSSS and DSSS with using black fiber and black dye were 3514 ml/m^2 and 3029 ml/m^2 at 2 cm water depth, respectively, with an increase of 16.01%. Also, it can be noticed that the CSSS has the best performance compared with the DSSS for the different proposed modifications. Table 1 summarizes the comparison of the actual and increases of the accumulated productivities of the tested CSSS and DSSS for the various conditions and modifications in the stills basin. From Table 1 it can be inferred that with using black fiber and black dye rather than fins, the accumulated productivity was increased by 40.67% for the CSSS. While, an increase of 44.58% was recorded for the same condition for the DSSS at 2 cm water depth.

The solar still thermal efficiency denotes the still capability in salt water desalinating. It can be used as a factor which must be maximized to get the best design of the solar still. Figs. 8 and 9 show the actual experimental hourly and daily thermal efficiency for the CSSS and DSSS tested stills for water depths of 2 cm, respectively. From Fig. 8, it can be seen that the hourly efficiencies for the CSSS were higher than of the DSSS for all the modified conditions of the basin. Also, it can observed that the significant values of the hourly

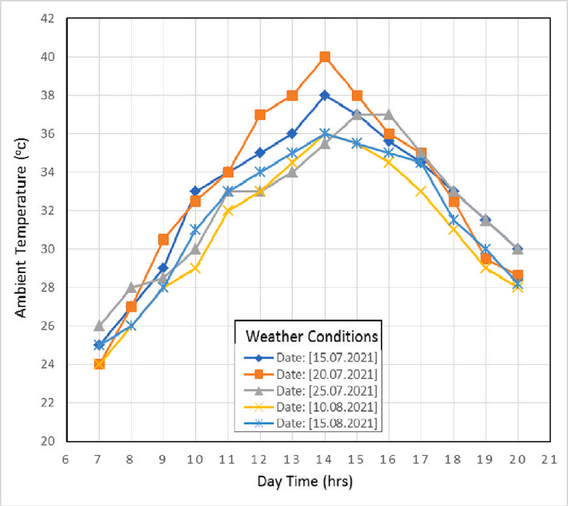

Fig. 5-B. Variations of ambient temperature through the experiments sunny days.

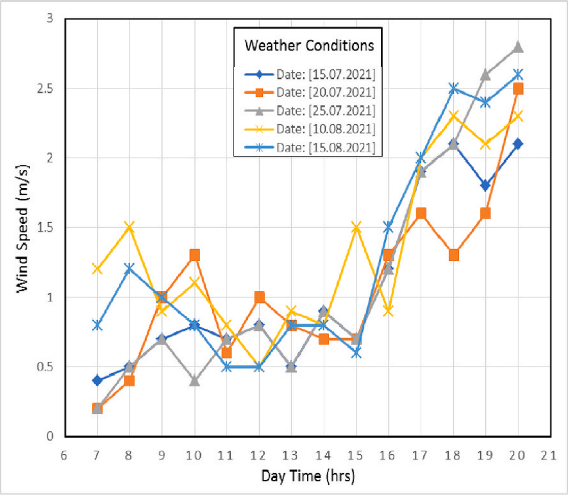

Fig. 5-C. Variations of wind speed through the experiments sunny days.

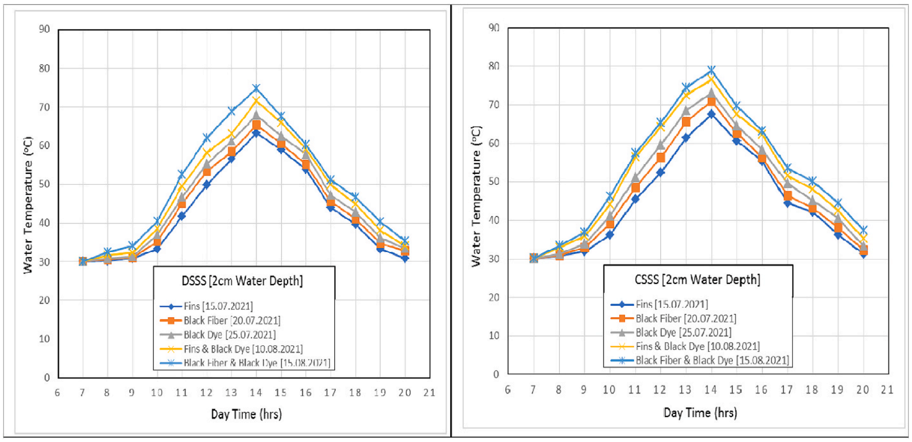

Fig. 6-A. Hourly variations of the water temperature for CSSS and DSSS with daytime for 2 cm water depth.

efficiency from mid-noon at 12:00 till 17:00 as the tested stills take some time to achieve the steady state conditions. This was because the global solar irradiation intensity was decreased and the capacity of thermal energy that led to high evaporation, and then the productivity was increased. After 18:00, the instant efficiency gets affected and the discussion of the hourly efficiency was focused through this period only. During the daytime, the greatest hourly efficiencies were 102.2, 114.4, 123.1, 133.3 and 149% for the CSSS, while these values were 81.9, 92.8, 97.2, 116.6 and 123.2% for the DSSS, for using fins, black natural-fiber, black dye, black dye with fins and black dye with black natural-fiber, respectively which occurred at 18:00. Fig. 9 depicts the variance in daily thermal efficiency as a function of the modified materials that used in the stills basin. As seen in the histogram, adding black dye with black natural-fiber to the both desalination systems improved the thermal performance significantly. The results clear that the actual daily thermal efficiency for the CSSS and DSSS with using black fiber and black dye were 30.42 and 26.32% at 2 cm water depth, respectively with an increased by 15.58%. Also, in all of the scenarios studied, the daily thermal efficiency of CSSS was greater than DSSS.

The analysis of economic for the CSSS and DSSS units were determined to evaluate the cost per liter of fresh water production. The investment principal was based on the each part prices of the distillation unit assembly, according to value of the Egyptian market. The economic analysis parameters and yields of the potable were tabulated and given in Table 2. The economic analysis results of the two tested stills were represents in Fig. 10 in order to compare between the CSSS and DSSS. From Table 2 and Fig. 10, it was clarified that the CPL of potable water produced for CSSS with using the black dye with black natural-fiber was about 0.0119 US$/L and the CPL for DSSS was about 0.0137 US$/L and the payback periods of CSSS and DSSS with using black fiber and black dye were 92 days and 106 days, respectively. While, for using the Fins only in the basin, the CPL for CSSS and DSSS were 0.0177 US$/L and 0.0209 US$/L. Also, the payback periods were raised to 140 days and 167 days, respectively.

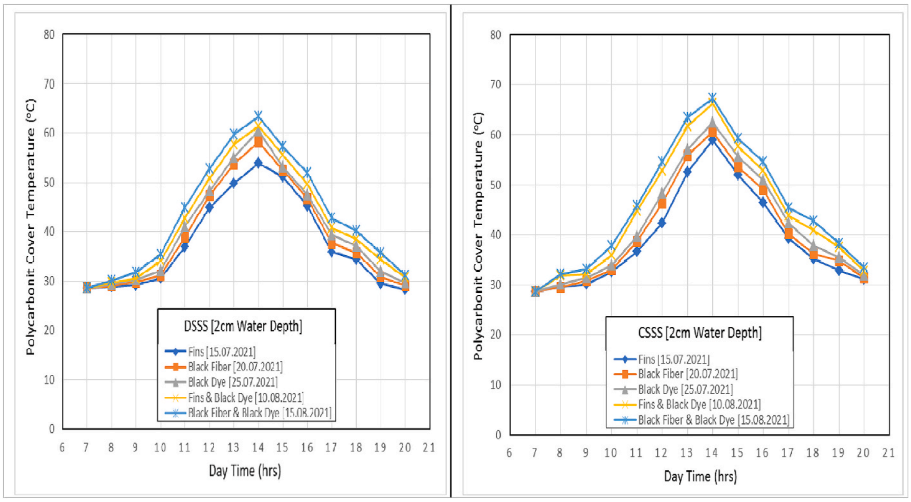

Fig. 6-B. Hourly variations of the polycarbonate cover temperatures for CSSS and DSSS with daytime at 2 cm water depth.

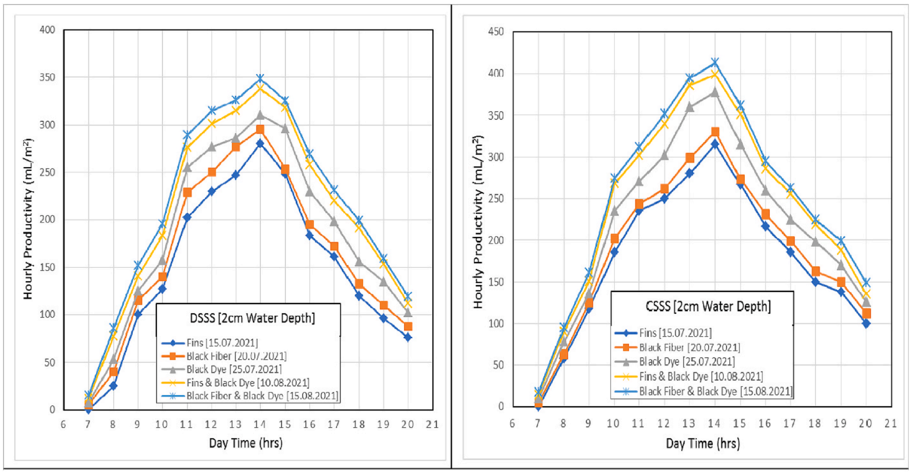

Fig. 7-A. Actual hourly variations of the productivity for CSSS and DSSS with daytime.

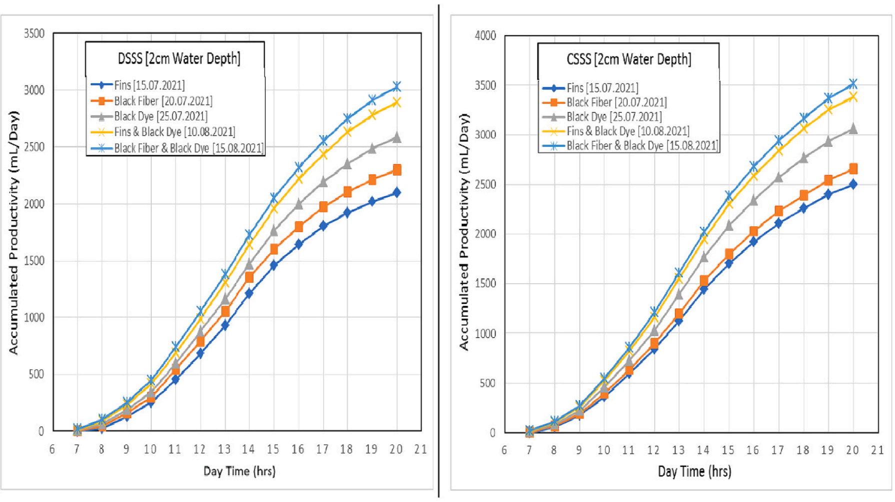

Fig. 7-B. Actual accumulated variations of the productivity for CSSS and DSSS with daytime.

Table 1

Comparison between the experimental daily yield for the tested CSSS and DSSS at the various conditions and modifications in stills basin.

Basin Condition	Daily yield [Accumulated productivity]				Increase % with DSSS
	CSSS		DSSS		
	(ml/m^2.day)	Increase %	(ml/m^2.day)	Increase %	
Fins	2498	Ref.	2095	Ref.	19.24
Black Fiber	2657	6.37	2301	9.83	15.47
Black Dye	3063	22.62	2588	23.53	18.35
Fins and Black Dye	3385	35.51	2895	38.19	16.93
Black Fiber and Black Dye	3514	40.67	3029	44.58	16.01

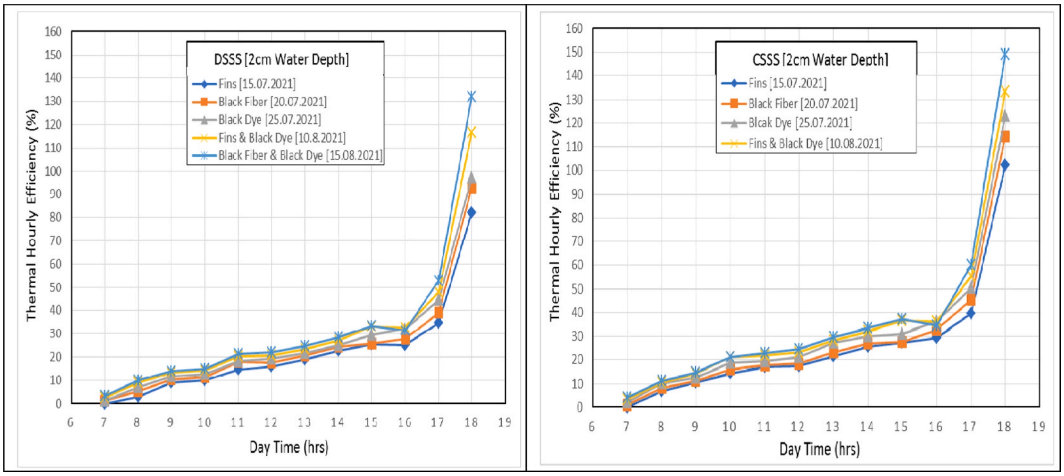

Fig. 8. Actual hourly thermal efficiency for CSSS and DSSS at 2 cm water depth.

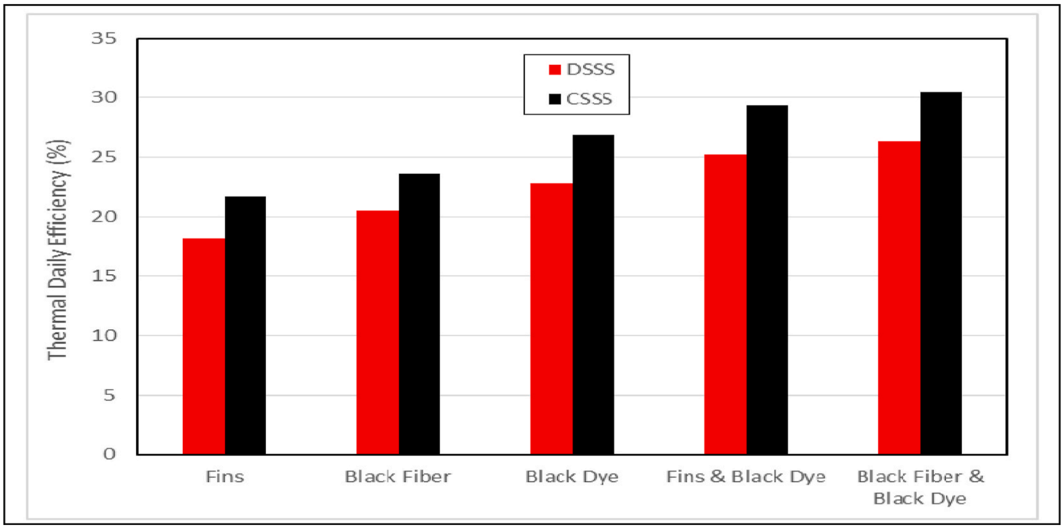

Fig. 9. Actual daily thermal efficiency for CSSS and DSSS at 2 cm water depth.

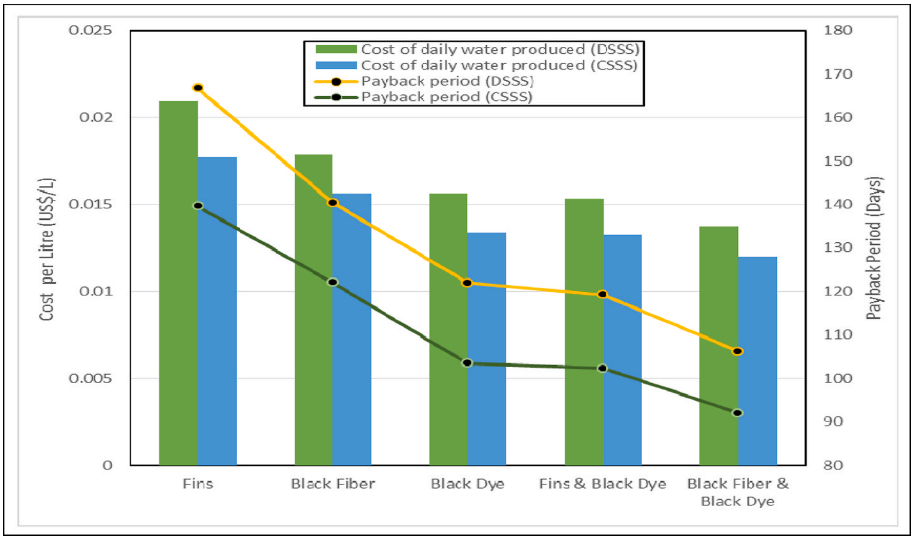

Fig. 10. Variations of CPL and payback periods for CSSS and DSSS at 2 cm water depth for various materials in the stills basin.

Table 2
Comparison of economic analysis parameters and outcomes of the tested CSSS and DSSS for the various conditions and modifications in stills basin.

Parameters	Fins		Black Fiber		Black Dye		Fins and Black Dye		Black Fiber and Black Dye	
	CSSS	DSSS	CSSS	DSSS	CSSS	DSSS	CSSS	DSSS	CSSS	DSSS
Useful life of the still	10									
The rate of interest (i)	12%									
No. of operated days in a years	335									
TFC - US$	81	80	76	75	75	74	82	81	77	76
FC-US$/year	14.34	14.16	13.45	13.27	13.27	13.10	14.51	14.34	13.63	13.45
MC-US$/year	1.43	1.42	1.35	1.33	1.33	1.31	1.45	1.43	1.36	1.35
AY-L/year	836.83	701.83	890.10	770.84	1026.11	866.98	1133.98	969.83	1177.19	1014.72
NF-US$/year	194.36	160.79	208.59	178.96	242.78	203.18	268.46	227.61	280.18	239.75
CPL-US$/L	0.0177	0.0209	0.0156	0.0178	0.0134	0.0156	0.0132	0.0153	0.0119	0.0137
PP- days	140	167	122	140	103	122	102	119	92	106

5. Conclusions

The cylindrical sector solar still (CSSS) and a double slope, single basin solar still (DSSS) have been designed, fabricated, and tested experimentally for 2 cm water depth and their performances under the Egyptian same weather conditions were compared. The CSSS and DSSS were tested with various materials, such as fins, black natural-fiber, black dye, black dye with fins and black dye with black natural-fiber along with seawater. The outcomes analysis obtained in this study led to draw the coming conclusions:

1. In all of the scenarios studied, the daily accumulated productivities, thermal efficiency of CSSS was greater than DSSS.
2. The experimental accumulated productivities of the CSSS and DSSS with using black fiber and black dye were 3514 ml/m^2 and 3029 ml/m^2.
3. The experimental accumulated productivity with using black fiber and black dye rather than fins was increased by 40.67% for the CSSS. While, an increased by 44.58% was recorded in the same condition for the DSSS.
4. The actual daily thermal efficiency of the CSSS and DSSS with using black fiber and black dye were 30.42 and 26.32%, respectively with an increased by 15.58%.
5. The CPL of potable water produced for CSSS with using the black dye and black natural-fiber was about 0.0119 US$/L, while it was about 0.0137 US$/L for DSSS with a reduction percentage of 13.13%.

Future studies

Based on the experience acquired through the present research, it is suggested for future work on this account; can add phase change materials and nanoparticles in the basins with sea water, as well as external reflectors to enhance the evaporation and condensation rates of studied stills; CSSS and DSSS.

CRediT Authorship Contribution statement

Mahmoud S. El-Sebaey: Designing and manufacturing the experimental setup, analyzing the results, and writing original draft. Asko Ellman: Analysis of the recorded data, review, and editing. Ahmed Hegazy: Analysis of the recorded data, analyzing the results and contributing to the scientific discussion. Fadl A. Essa: Analysis of the recorded data, review, and editing.

Declaration of competing interest

The authors declare that they have no known competing financial interests or personal relationships that could have appeared to influence the work reported in this paper.

Data availability

Data will be made available on request.

Nomenclature

Variable	*Definition*	*Unit*
C_b	Basin liner specific heat	J/kg.°C
C_{pc}	Specific heat of polycarbonate cover	J/kg.°C
C_w	Water specific heat	J/kg.°C
FF	Fund sinking factor	–
$h_{c,b-w}$	Basin to water convective coefficient of heat transfer	W/m^2.°C
$H_b(t)$	Basin absorbed solar radiation fraction	W/m^2
$H_{pc}(t)$	Polycarbonate cover solar radiation absorbed fraction	W/m^2
$H_w(t)$	Water solar radiation absorbed fraction	W/m^2
i	Interest rate	%
i_s	Solar still lifetime	years
k_w	Water thermal conductivity	W/m.K
L_w	Water basin characteristic length	m
m_b	Basin liner mass	kg
m_{pc}	polycarbonate cover mass	kg
m_w	Water mass	kg
P	Principal investment	%
q_{b-a}	Basin to the ambient heat loss	W/m^2
$q_{c,b-w}$	Basin to water convective rate of heat transfer	W/m^2
$q_{c,pc-a}$	Polycarbonate cover to the ambient convective rate of heat transfer	W/m^2
q_{cw}	Water to polycarbonate cover convective rate of heat transfer	W/m^2
q_{ew}	Water to polycarbonate cover evaporative rate of heat transfer	W/m^2
q_{rw}	Water to polycarbonate cover radiative rate of heat transfer	W/m^2
$q_{r,pc-sky}$	Polycarbonate cover to sky radiative rate of heat transfer	W/m^2
Ra_w	Water rayleigh number	–
S	Salvage value	%
T_b	Basin liner temperature	°C
T_{pc}	Polycarbonate cover temperature	°C
T_w	Water temperature	°C

Abbreviations

DSSS	Double Slope Solar Still
CSSS	Cylindrical Sector solar still
TFC	Total Fixed Cost
PPM	Parts Per Million
TDS	Total Dissolved Solids
UNICEF	United Nations Children's Emergency Fund
SODY	Still Operating Days per Year

References

[1] Subbarama Kousik Suraparaju, Ragupathy Dhanusuraman, Sendhil Kumar Natarajan, Performance evaluation of single slope solar still with novel pond fibres, Process Saf. Environ. Protect. 154 (2021) 142–154.
[2] Swellam W. Sharshir, A.W. Kandeal, Youssef M. Ellakany, Ibrahem Maher, Khalil Ahmed, Swidan Ahmed, Gamal B. Abdelaziz, Hany Koheil and Maher Rashad, Improving the performance of tubular solar still integrated with drilled carbonized wood and carbon black thin film evaporation, Sol. Energy 233 (2022) 504–514.
[3] Mahmoud S. El-Sebaey, Hegazy Ahmed, Asko Ellman, Tarek Ghonim, "Experimental and CFD study on single slope double basin solar still", ERJ, PART 1, Mach. Eng., January 44 (1) (2021) 21–32.
[4] Raj Vardhan Patel, b Kiran Bharti, Gaurav Singh, Gaurav Mittal, Desh Bandhu Singh, Anshul Yadav, Comparative investigation of double slope solar still by incorporating different types of collectors: a mini review, Mater. Today: Proc. 38 (2021) 300–304.
[5] Bahaa Saleh, Fadl A. Essa, Zakaria Omara, Mohamed H. Ahmed, S. Mahmoud, El-Sebaey, Using direct solar energy conversion in distillation via evacuated solar tube with and without nanomaterials, Processes 11 (2023) 1734.
[6] Duc-Trung Tran, Julie Mendret, Jean-Pierre Méricq, Catherine Faur, Stephan Brosillon, Performance of PVDF-TiO_2 membranes during photo-filtration in the presence of inorganic and organic components, membranes, MDPI 12 (2) (2022) 245.
[7] G.B. Abdelaziz, M.A. Dahab, M.A. Omara, S.W. Sharshir, A.M. Elsaid, E.M.S. El-Said, Humidification dehumidification saline water desalination system utilizinghigh frequency ultrasonic humidifier and solar heated air stream, Therm. Sci. Eng. Prog. 27 (2022), 101144.
[8] M. Abd Elaziz, F. Essa, A.H. Elsheikh, Utilization of ensemble random vector functional link network for freshwater prediction of active solar stills with nanoparticles, Sustain. Energy Technol. Assessments 47 (2021), 101405.
[9] F.A. Essa, Wissam H. Alawee, Suha A. Mohammed, Hayder A. Dhahad, A.S. Abdullah, Z.M. Omara, Experimental investigation of convex tubular solar still performance using wick and nanocomposites, Case Stud. Therm. Eng. 27 (2021), 101368.
[10] H. Al-Hinai, M. Al-Nassri, B. Jubran, Effect of climatic, design and operational parameters on the yield of a simple solar still, Energy Convers. Manag. 43 (13) (2002) 1639–1650.
[11] Mahmoud S. El-Sebaey, Asko Ellman, Hegazy Ahmed, Tarek Ghonim, Experimental analysis and CFD modeling for conventional basin-type solar still, energies, MDPI 13 (2020) 5734.
[12] Suresh Kumar Patel, Brajesh Kumar, Production of potable water from Gomti River by using modified double slope solar still with external mounted reflectors, Sol. Energy 209 (2020) 576–589.
[13] Mahmoud S. El-Sebaey, Asko Ellman, Hegazy Ahmed, Hitesh Panchal, Experimental study and mathematical model development for the effect of water depth on water production of a modified basin solar still, Case Stud. Therm. Eng. 33 (2022), 101925.
[14] A.A. El-Sebaii, Thermal performance of a triple-basin solar still, Desalination 174 (2005) 23–37.
[15] M.E.H. Attia, et al., Enhancement of hemispherical solar still productivity using iron, zinc and copper trays, Sol. Energy 216 (2021) 295–302.
[16] K.V. Modi, K.H. Nayi, S.S. Sharma, Influence of water mass on the performance of spherical basin solar still integrated with parabolic reflector, Groundwater for Sustainable Development 10 (2020), 100299.
[17] W.H. Alawee, et al., Improving the performance of pyramid solar still using rotating four cylinders and three electric heaters, Process Saf. Environ. Protect. 148 (2021) 950–958.
[18] H. Al-Madhhachi, G.F. Smaisim, Experimental and numerical investigations with environmental impacts of affordable square pyramid solar still, Sol. Energy 216 (2021) 303–314.
[19] Swellam W. Sharshir, A.W. Kandeal, Improving the performance of tubular solar still integrated with drilled carbonized wood and carbon black thin film evaporation, Sol. Energy 233 (2022) 504–514.
[20] T. Rajaseenivasan, K. Kalidasa Murugavel, T. Elango, R.A. Samuel Hansen, Review of different methods to enhance the productivity of the multi-effect solar still, Renew. Sustain. Energy Rev. 17 (2013) 248–259.
[21] A.E. Kabeel, A. Khalil, Z.M. Omara, M.M. Younes, Theoretical and experimental parametric study of modified stepped solar still, Desalination 289 (2012) 12–20.
[22] Y.A.F. El-Samadony, A.S. Abdullah, Z.M. Omara, Experimental study of stepped solar still integrated with reflectors and external condenser, Exp. Heat Tran. 28 (2015) 392–404.
[23] A.S. Abdullah, et al., Improving the trays solar still performance using reflectors and phase change material with nanoparticles, J. Energy Storage 31 (2020), 101744.
[24] H. Panchal, et al., Experimental investigation on the yield of solar still using manganese oxide nanoparticles coated absorber, Case Stud. Therm. Eng. 25 (2021), 100905.
[25] P.N. Kumar, et al., Experimental investigation on the effect of water mass in triangular pyramid solar still integrated to inclined solar still, Groundwater for Sustainable Development 5 (2017) 229–234.
[26] Z.M. Omara, et al., Experimental investigation of corrugated absorber solar still with wick and reflectors, Desalination 381 (2016) 111–116.
[27] A. Abdullah, et al., Rotating-wick solar still with mended evaporation technics: experimental approach, Alex. Eng. J. 58 (4) (2019) 1449–1459.
[28] F.A. Essa, A.S. Abdullah, Experimental enhancement of tubular solar still performance using rotating cylinder, nanoparticles' coating, parabolic solar concentrator, and phase change material, Case Stud. Therm. Eng. 29 (2022).
[29] Hitesh Panchal, Heri Nurdiyanto, Kishor Kumar Sadasivuni, Sanil S. Hishan, F.A. Essa, Mohammad Khalid, Swapnil Dharaskar, S. Shanmugan, Experimental investigation on the yield of solar still using manganese oxide nanoparticles coated absorber, Case Stud. Therm. Eng. 25 (2021), 100905.
[30] P. Valsaraj, An experimental study on solar distillation in a single slope basin still by surface heating the water mass, Renew. Energy 25 (4) (2002) 607–612.
[31] H. Panchal, et al., Enhancement of the yield of solar still with the use of solar pond: a review, Heat Transfer 50 (2) (2021) 1392–1409.
[32] K.V. Modi, D.L. Shukla, Regeneration of liquid desiccant for solar air conditioning and desalination using hybrid solar still, Energy Convers. Manag. 171 (2018) 1598–1616.
[33] S. Sharshir, et al., The effects of flake graphite nanoparticles, phase change material, and film cooling on the solar still performance, Appl. Energy 191 (2017) 358–366.
[34] Z. Omara, et al., The cooling techniques of the solar stills' glass covers–a review, Renew. Sustain. Energy Rev. 78 (2017) 176–193.
[35] S. Abdallah, M.M. Abu-Khader, O. Badran, Effect of various absorbing materials on the thermal performance of solar stills, Desalination 242 (1–3) (2009) 128–137.
[36] A.S. Abdullah, et al., Enhancing the solar still performance using reflectors and sliding-wick belt, Sol. Energy 214 (2021) 268–279.
[37] Z.M. Omara, M.H. Hamed, A. Kabeel, Performance of finned and corrugated absorbers solar stills under Egyptian conditions, Desalination 277 (1–3) (2011) 281–287.
[38] M. Dubey, D.R. Mishra, Experimental analysis of double slope solar still augmented with dye, pebbles and metal chips, Environ. Sci. Pollut. Control Ser. 28 (17) (2021) 22077–22090.
[39] Z.M. Omara, et al., Experimental investigation of corrugated absorber solar still with wick and reflectors, Desalination 381 (2016) 111–116.
[40] B.H. Upadhyay, et al., Design, development and techno economic analysis of novel parabolic trough collector for low-temperature water heating applications, Case Stud. Therm. Eng. 26 (2021), 100978.
[41] S. Abdallah, O. Badran, Sun tracking system for productivity enhancement of solar still, Desalination 220 (1–3) (2008) 669–676.
[42] Mahmoud S. El-Sebaey, et al., A case study on thermal performance analysis of a solar still basin employing ceramic magnets, Case Stud. Therm. Eng. (2022), 102402.
[43] L. Malaeb, G.M. Ayoub, M. Al-Hindi, The Effect of Cover Geometry on the Productivity of a Modified Solar Still Desalination Unit, Energy Procedia, 2014, pp. 406–413.
[44] A.A. El-Sebaii, M. El-Naggar, Year round performance and cost analysis of a finned single basin solar still, Appl. Therm. Eng. (2017) 787–794.

[45] H. Moungar, A. Azzi, Y. Sahli, A. Hieda, University Politehnica of Bucharest Scientific Bulletin Series c-Electrical Engineering and computer Science, 2018, pp. 2286–3540.
[46] M. El-Naggar, A.A. El-Sebaii, M.R. Ramadan, S.A. Enein, Experimental and theoretical performance of finned-single effect solar still, Desalination Water Treat. (2015) 1–16.
[47] K. Rabhi, R. Nciri, F. Nasri, C. Ali, H.B. Bacha, Experimental performance analysis of a modified single-basin single-slope solar still with pin fins absorber and condenser, Desalination (2017) 86–93.
[48] R. Dhivagar, M. Mohanraj, Performance Improvements of Single Slope Solar Still Using Graphite Plate Fins and Magnets, Environmental Science and Pollution Research, 2021.
[49] V.K. Chauhan, S.K. Shukla, P.K.S. Rathore, A systematic review for performance augmentation of solar still with heat storage materials: a state of art, J. Energy Storage 47 (2022), 103578.
[50] Fayadh M. Abed, Ahmed H. Ahmed, M. Hasanuzzaman, Laveet Kumar, Nasur M. Hamaad, Experimental investigation on the effect of using chemical dyes on the performance of single-slope passive solar still, Sol. Energy 233 (2022) 71–83.
[51] ApurbaLayek, Exergetic analysis of basin type solar still, Engineering Science and Technology, Int. J. 21 (2018) 99–106.
[52] V.K. Dwivedi, G.N. Tiwari, Experimental validation of thermal model of a double slope active solar still under natural circulation mode, Desalination (2010) 49–55.
[53] I. Altarawneh, S. Rawadieh, M. Batiha, L. Al-Makhadmeh, S. Alrowwad, M. Tarawneh, Experimental and numerical performance analysis and optimization of single slope, double slope and pyramidal shaped solar stills, Desalination (2017) 124–134.
[54] T. Elango, K.K. Murugavel, The effect of the water depth on the productivity for single and double basin double slope glass solar stills, Desalination (2015) 82–91.
[55] Ali Omran Al-Sulttani, Amimul Ahsan, Heat transfer coefficients and yield analysis of a double-slope solar still hybrid with rubber scrapers: an experimental and theoretical study, Desalination 407 (2017) 61–74.
[56] V. Velmurugan, C.K. Deenadayalan, H. Vinod, K. Srithar, Desalination of effluent using fin type solar still, Energy 33 (2008) 1719–1727.
[57] G.N. Tiwari, L. Sahota, Review on the energy and economic efficiencies of passive and active solar distillation systems, Desalination 401 (2017) 151–179.
[58] S. Kousik, R. Dhanusuraman, S. Natarajana, Performance evaluation of single slope solar still with novel pond fibres, Process Saf. Environ. Protect. 154 (2021) 142–154.